**Proceedings of the**
**International Conference on Mechanical Engineering and Renewable Energy 2013**
**(ICMERE2013) 1-3 May 2014, Chittagong, Bangladesh**

**ICMERE2013-PI-243**

# FRACTURE PROPERTIES OF THIN PAPERS MADE FROM GRAPHENE OXIDE

**Md. Nizam Uddin [1], Md. Ashraful Islam [2] and Mohammad Mashud [3]**

[1-3]Department of Mechanical Engineering, Khulna University of Engineering and Technology (KUET), Khulna-9203, Bangladesh.
[1,*]engrnizam02@gmail.com, [2]ashraf.bitr@gmail.com, [3]mdmashud@yahoo.com

***Abstract***- *Measurements are reported of the fracture toughness of graphene oxide (GO) papers. The concept of Linear Elastic fracture mechanics (LEFM) is applied to measure the fracture toughness of GO papers. The effects of GO sizes on fracture toughness are studied. GO sheets prepared by modified Hummers method are sorted into four different groups by centrifugation and through vacuum filtration, GO papers of different sheet sizes are prepared. GO papers made from large sheets give higher fracture toughness than those made from small GO sheets. About 66% enhancement of fracture toughness are observed. The failure mechanisms taking place during the fracture toughness tests are identified from the microscopic examination of the fracture surfaces. Cleavage failure is the dominant failure mechanisms under mode-I loading of GO papers.*

**Keywords:** Graphene oxide paper, Fracture toughness, Cleavage failure, Vacuum filtration.

## 1. Introduction

Since its discovery in 2004 [1], graphene - the parents of all graphitic materials has become one of the most exciting topics of research in the last few years. Graphene consists of one atom thick $sp^2$ bonded carbon atoms arranged in a honeycomb lattice structure, and have exceptionally high in-plane electronic mobility, mechanical strength and thermal conductivity [2-6]. Among different methods for the fabrication of graphene based materials, graphene oxide (GO) synthesized from oxidation of graphite is the most versatile method [7]. GO is an atomic sheet of graphite containing several oxygenated functional groups on its basal planes and at its edges, which form a hybrid structure of $sp^2$ and $sp^3$ hybridized carbon atoms [8]. Both the basal plane and edges of GO oxygenated functional groups are covalently bonded, namely hydroxyl and epoxy groups on the basal plane and carboxylic, carbonyl acid groups are at the edges [9] provide well dispersed individual GO sheets in water and organic solvents [10-11]. It is widely used as a building block in composites, mechanical actuators, nano-robots and paper like materials, energy related materials, biological and medical applications [12-13]. In recent years, graphene-based paper materials have attracted much interest because of their outstanding strength, stiffness and high degree of flexibility [8, 14]. This paper-like material may be used as sealants, actuators, bio-compatible substrates, flexible substrates with high chemical and thermal stability. GO paper, a free standing layer by layer hierarchical structure is fabricated from aqueous GO dispersion via vacuum-assisted self-assembly technique. The mechanical properties of GO papers like tensile strength and Young's modulus have been extensively studied [8, 13]. The lateral dimensions of GO sheets have significant impact in controlling their properties and applications. Large and small GO sheets are ideally suited in a variety of applications. For example, for bio sensing and drug delivery [15-16] small GO sheets and polymer based composites [17], optoelectronic devices [18] large GO sheets with controlled sizes are preferable. Various methods are proposed and used in literature for the size controlled synthesized of GO sheets [19-20]. In this study repeated centrifugation is used to sort as produced GO sheets into four different sizes.

Fracture toughness is the ability of a material to resist the propagation of a pre-existing flaw or crack. It is a generic term which measured the resistance to propagation of a crack. It is a fundamental material property like elastic modulus, tensile strength etc. For bulk materials and relatively thick films fracture toughness can be measured using ASTM standards [21]. In case of thin films, fracture toughness evaluation is quiet difficult due to thickness limitation using ASTM standards [22]. However, until now, there is no standard procedure for evaluation of fracture toughness under plane stress condition. Free-standing paper or foil like materials are used in various engineering applications and their fracture toughness evaluation becomes essential. The concept of Linear Elastic fracture mechanics (LEFM) is applied to measure the fracture toughness of GO paper. The linear elastic fracture mechanics approach based on the hypothesis that material will behave as a pure linear elastic materials. It has two main approaches. One is

based on Griffith fracture theory and the other approach is based on mathematical characterization of the crack tip stress field- stress intensity factor approach. The stress intensity factor describes the state of the stress at the vicinity of the crack tip while considering the applied load, specimen geometry and crack geometry. This works aims the evaluation of the fracture properties of GO papers in mode-I loading. Experiments were performed to determine the fracture toughness of GO papers. In addition, the study specially focuses on the effect of GO sheet sizes on the fracture properties of GO papers.

## 2. Experimental

### *2.1 Synthesis of GO*

GO was prepared from purified natural graphite flakes (Asbury Graphite Mills) based on modified chemical method [23-24]. In a typical experiment 5 g of natural graphite flakes (Asbury Graphite Mills, US) and 150 ml sulfuric acid ($H_2SO_4$, 95.5-96.5%, General Chemical) were first mixed and stirred in a round bottom flask at a speed of 200 rpm. 50 ml of fuming nitric acid ($HNO_3$, Fisher) was then added into the mixture. The mixture was kept at room temperature and stirred for 24 h. 200 ml of de-ionized water was then poured slowly into the mixture. The resultant mixture was washed using DI water three times and centrifugation, which was then dried at 60°C for 24 hr to obtain GIC. The dry GIC powder was thermally expanded at 1050 °C for 15sec. The expanded graphite (EG) was then used for the production of GO sheets. 0.5 g of EG and 100 ml of sulfuric acid ($H_2SO_4$, 95.5-96.5%, General Chemical) were mixed and stirred in a three neck flask. Next, 5 g of $KMnO_4$ was drop-wise added to the mixture while stirring. The mixture was then stirred at 60°C for 24 h. The solution was transferred into an ice bath, and 100 ml of de-ionized water and 25ml of $H_2O_2$ were poured slowly into the mixture to find the colour of the suspension to change into light brown. Having stirred for another 30 min, the GO particles were then washed and centrifuged with HCl solution (9:1 vol water: HCl) three times, then centrifuged again and washed with de-ionized water until the pH of the solution became about 5 to 6. The obtained GO particles were then diluted using DI water (~1 mg/ml) and then sonicated for 20min using a bath sonicator.

### *2.2 Sorting of GO sheets into large GO and small GO*

The as prepared GO dispersion in water has different sizes of monolayer GO sheets. Unsorted GO solution was separated into four different groups with uniform sizes through three-step centrifugation on a table-top centrifuge (SIGMA 2-16P) as shown in Fig. 1. At first the unsorted GO dispersion was centrifuged at 8000 rpm for 40 min producing supernatant and precipitate. The supernatant and precipitate was collected. This supernatant was marked as small GO and the precipitate was dispersed in water and centrifuged at 6000 rpm for 50 min, again producing supernatant (large GO) and precipitate. The precipitate was dispersed in water again and centrifuged at 4000 rpm for 60 min producing supernatant (very large GO) and precipitate (ULGO). In this study only ultra large GO (ULGO) and small GO were used for the fabrication of Large GO and Small GO papers. According to our recent report the sizes of small GO and ULGO ranging from several to a couple of hundreds of µm [25].

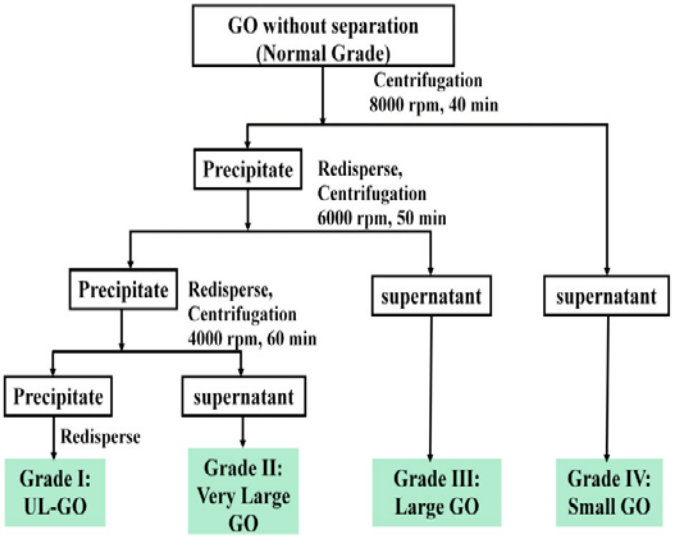


Fig. 1: Flow charts for separation of unsorted GO into four grade: ULGO, very large GO, large GO and small GO by three steps centrifugation

### *2.3 Fabrication of GO papers*

GO paper was fabricated by flow-directed vacuum filtration of aqueous GO dispersions through a Millipore filter membrane (90 mm in diameter and 0.22 µm pore size) followed by air drying and peeling off from the filter paper as shown in Fig.2. The thickness of each paper is controlled by adjusting volume of the aqueous GO dispersions. For the fracture toughness testing specimen, the thickness of the paper was about 20±0.001µm. All the specimens were dried in an oven at 60°C for seven days to achieve low moisture content before testing.

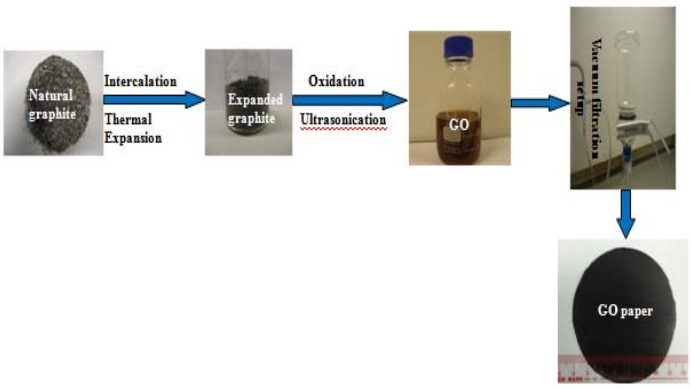


Fig. 2: Process flow chart for the fabrication of GO paper

*2.4 Characterization and mechanical tests*

There is no standard procedure or commonly accepted methodology for evaluation of fracture toughness under plane stress condition but two conditions are necessary. Firstly when materials fail, the stress acting over the un-cracked region should be less than the yield stress of the material [26]. Secondly appropriate dimensions of the specimen so that boundaries do not interfere with the crack tip stress distribution [27]. By using a desirable crack length and large enough specimen these condition can be met. For different materials and specimen geometry, these dimensions are different. A DENT specimen was prepared for the fracture toughness testing of different paper materials as shown in Fig. 3. The width of the specimen was varied from 2b = 5 to 30mm, height to width ratio h/b = 2 and crack length to width ratio a/b= 0.15 to 0.69. The edge cracks were made with a sharp surgical blade. The testing was conducted on a universal testing machine (Alliance RT/5) at a cross head speed of 1mm/min. The fracture toughness was calculated using the following equations (1) and (2). For an elastic specimen containing a crack and under a critical tensile stress $\sigma_C$ (at which instability occurs) the critical stress intensity factor $K_C$ in the plane stress mode-I is given by [28]

$$K_C = \sigma_C \sqrt{\pi a}\, F\left(a/b\right) \quad (1)$$

Where, crack length at instability is $a$, $F\left(a/b\right)$ is a finite-width correction factor and for an infinite plates its unity. According to Brown (1966) for a double edge notch tension specimen this geometric correction factor is

$$F\left(a/b\right) = 1.12 + 0.203\left(a/b\right) - 1.197\left(a/b\right)^2 + 1.93\left(a/b\right)^3 \quad (2)$$

The peak load from the load-extension curve and initial crack length were used for the calculation of $K_C$ as there was no substantial crack growth occurs before catastrophic failure of different types of paper materials studied here.

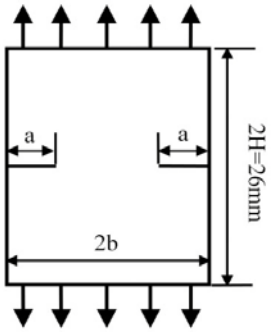


Fig. 3: Double edge notched tension specimen

The cross-sectional morphology of the fracture surfaces were examined on a scanning electron microscope (SEM, JEOL 6700F, JSM).The Raman spectroscopy (Reinshaw Micro Raman/ Photoluminescence System) was used to analyze the structure of GO papers using 633 nm He-Ne laser. X-ray diffraction measurements were conducted using a high resolution X-ray diffraction system (XRD, PW1825, Philips) operating with Cu $K_\alpha$ radiation ($\lambda$ = 1.5406 Å) in the 2-theta (2θ) range from 5–40° at a scanning rate of 2° $min^{-1}$.

## 3. Results and Discussion

### 3.1 Surface chemistry

Raman spectroscopy is a powerful nondestructive tool for the analysis of ordered and disordered crystal structures of carbon. Fig.4 shows the Raman spectra of Small GO, unsorted GO and Large GO papers and the corresponding $I_D/I_G$ intensity ratio. The G band (at ~1590 $m^{-1}$) is Raman active for $sp^2$-hybridized carbon-carbon bonds in graphene [29-31]. While D band (at ~1354 $cm^{-1}$) is associated with the presence of defects in the graphite material such as bond-angle disorder, bond-length disorder, vacancies, edge defects, etc. [32]. The intensity ratio $I_D/I_G$ is widely used to measure the defects quantity in graphitic materials [33]. The Raman spectra shows an increase in the D/G intensity ratio from 2.02 for Large GO to 2.43 for small GO paper, clearly indicate the increased defects quantity in small GO sheets.

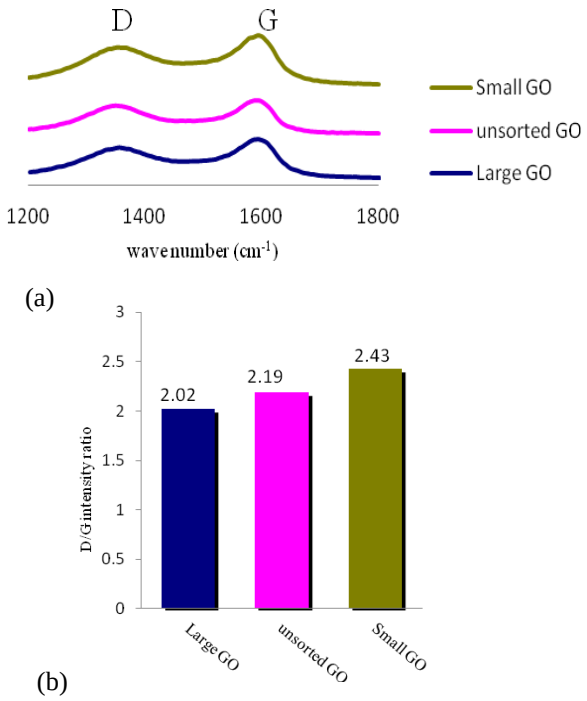


Fig. 4: Raman spectra of Small, unsorted and Large GO papers (a) D- and G-band peaks and (b) $I_D/I_G$ intensity ratio of Small, unsorted and Large GO papers.

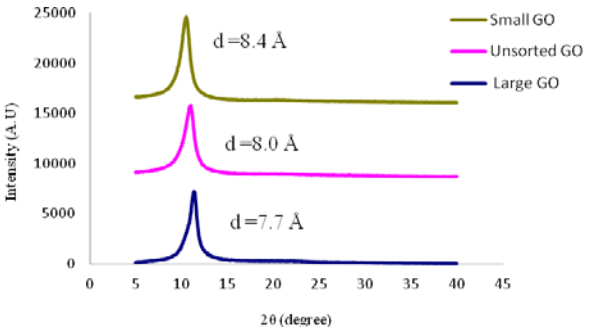


Fig. 5: X-ray diffraction patterns of Small, unsorted and Large GO papers

The XRD pattern (Fig.5) of Small, unsorted and Large GO papers exhibits a characteristic XRD peak at 2θ = 10.53º, 11.03º and 11.35° corresponding to a distance of 8.4 Å , 8.0 Å and 7.7Å between the stacked GO sheets. Small GO papers have higher layer to layer distance than Large GO papers. Large GO sheets have higher C/O ratio and Small GO contained more oxygenated functional groups for a given area of materials [25]. Thus, Small GO with more oxygenated functional groups absorbing more water through hydrogen bonding leading higher layer to layer distance (d-spacing).

*3.2 Fracture properties of unsorted GO papers*

The effect of initial crack length on fracture toughness was investigated. The width of the specimen is constant (13mm) and the crack length is varied between 2 mm and 9 mm. Fig.6. shows the effect of the ratio of initial crack length to specimen width, $a/b$ on fracture toughness of unsorted GO paper for constant specimen width. Fracture toughness appears to be maximum for $a/b$ in the range of 0.38 and 0.46. This follows the theoretical predicted optimum $a/b$ of $1/3$. Theoretically release of strain energy with crack extension to be maximum for $a/b$ of $1/3$ [34]. Fracture toughness values decreases with increasing initial crack length to specimen width ratio especially for $a/b$ of 0.61, 0.69. This is because for complete fracture strain energy in the system in not adequate due to narrow un-cracked width.

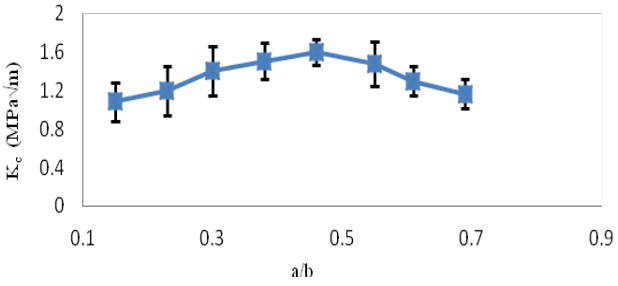


Fig. 6: Effect of initial crack length to specimen width, a/b, (width 13mm) on fracture toughness of GO paper.

For constant initial crack length to width ratio $a/b$ of 0.38 and 0.46, the effect of specimen width $2b$, on fracture toughness are shown in Fig. 7. Fracture toughness appears to be level off at a specimen width of about 10mm. Using molecular-dynamics simulation the fracture toughness of single layer graphite sheet was found to be 4.7 MPa√m [35].

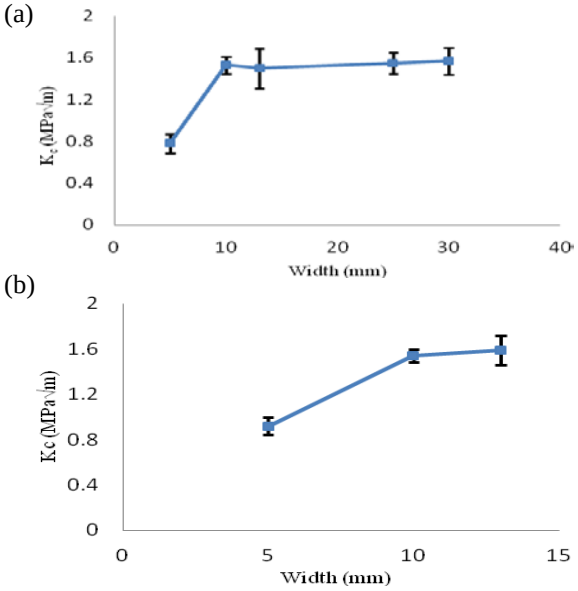


Fig. 7: Effect of specimen width 2b on fracture toughness of GO paper, (a) crack length to width ratio a/b = 0.38 and (b) a/b = 0.46

*3.3 Morphology and effect of GO sheets sizes on fracture properties of GO papers*

GO sheets were sorted as Small GO and Large GO sheets and the effect of GO sheets size on fracture properties were investigated. Representative load-extension curves obtained from the fracture toughness tests of three different kinds of GO papers are shown in Fig.8.(a)

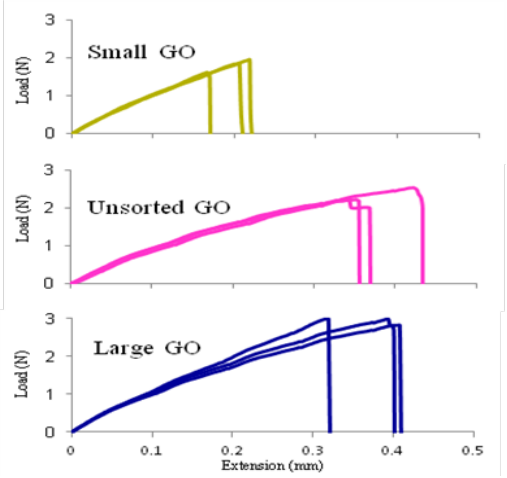


(a)

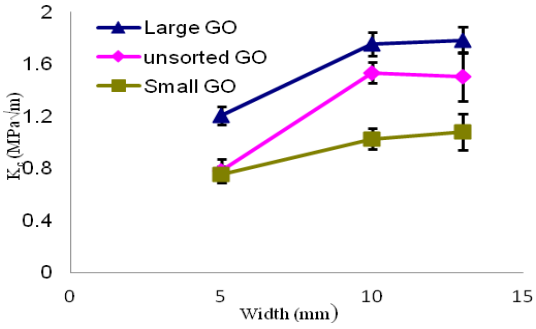


(b)

Fig. 8: (a) Load- extension curves and (b) Comparison of the fracture toughness; of Small, unsorted and Large GO papers crack length to width ratio *a*/b = 0.38, width 13mm

From Fig. 8(a) load increased almost linearly with extension when crack initiated until it reached the maximum where catastrophic failure occur. This means that fracture of GO paper like a brittle material. From the load-extension curves of three different types of GO paper, it shows that comparatively higher load is necessary for the failure occurs in case of Large paper as compared to unsorted GO and Small GO paper. Fig. 8(b) exhibits the comparison of the fracture toughness of of Small, unsorted and Large GO papers for constant initial crack length to width ratio $^{a}/_{b}$ of 0.38 for different specimen width. It appears that about 66% enhancement of the fracture toughness as paper made from Large GO sheets than those from Small GO sheets. There are several factors that enhance the fracture toughness of GO paper i.e. GO sheet size, stacking order of GO layer, defects and voids in the GO, overlapping size of GO layers, layer-by-layer hierarchy [36]. From the Raman spectra (Fig.4) it is found that Large GO sheets contain fewer defects than small GO sheets as $I_D/I_G$ intensity ratio are lower for the Large GO paper than small GO paper. Also from X-ray diffraction analysis (Fig.5) the interlayer distance of Large GO paper are lower than the Small GO paper. Small GO sheets contain more oxygenated functional group and through hydrogen bonding it could absorb more water leading higher layer to layer distance (d-spacing). The GO paper prepared from Large GO sheets exhibit more compact structure and better alignment during self-assembly process [37]. GO paper assembled in a layer-by-layer hierarchy where GO sheets are bridged on the edges (intralayer) and adjacent graphene sheets (interlayer) through *sp*2 carbon-carbon covalent bonds, hydrogen bonds, van der Waals forces. The failure mechanisms taking place during the fracture toughness test were evaluated for three different types of GO papers from the cross-sectional fracture surface. The fracture surfaces were examined using SEM and typical photographs taken halfway to the specimen edge are presented in Fig.9. From which typical failure mechanism can be identified. From observations of fracture surfaces of three different types of GO papers, a well packed layer structure was clearly demonstrated. It is interesting to note that when tensile load is applied to GO paper having pre-crack, once the load reaches a certain critical level fracture of the sheet was initiated by cleavage of the GO sheets and crack propagates perpendicular to the loading direction indicating a brittle, catastrophic failure. Crack followed a straight path without any deflection. The *sp*2 carbon-carbon covalent bonds are short-ranged and the deformation of GO sheets generally involves the localized processes of bond breaking. The fracture surfaces of unsorted GO and Large GO paper displayed a smooth and featureless surface and well bonded GO sheets while small GO paper exhibits some sort of pullout (de-bonding) of small GO sheets. This means that fracture mechanisms of unsorted GO and Large GO papers are dominated by cleavage failure under mode-I loading while in Small GO paper both cleavage and de-bonding of the GO sheets.

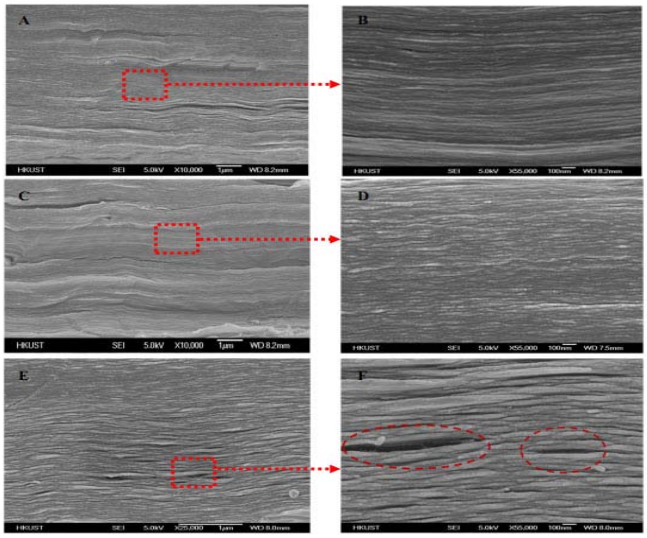


Fig. 9: The SEM photographs of the fracture surfaces of GO paper (A-B) unsorted GO, (C-D)Large GO and (E-F) Small GO at low and high magnification

## 4. Conclusions

The fracture toughness of GO papers was measured. The effects of GO sheets sizes on fracture toughness were evaluated. An easy and efficient centrifugation based sorting process was used to separate large GO and small GO sheets. GO paper made from Large GO sheet gives higher fracture toughness than those from small GO sheets. About 66% enhancement of fracture was observed. The failure mechanisms taking place during the fracture toughness tests are identified from the microscopic examination of the fracture surfaces. Cleavage failure is the dominant failure mechanisms under mode-I loading of GO papers.

## References

[1] K.S. Novoselov, A.K. Geim, S.V. Morozov, D. Jiang, Y. Zhang, S.V. Dubonos, V. Grigorieva, A.A. Firsov, Electric field effect in atomically thin carbon films, Science, 306, 666-669, 2004.

[2] K.S. Novoselov, A.K. Geim, S.V. Morozov, D. Jiang, M.I. Katsnelson, S.V. Dubonos, A.A. Firsov, Two dimensional gas of mass less dirac fermions in graphene, Nature, 438, 197–200, 2005.

[3] A.K. Geim, K.S. Novoselov, The rise of graphene,

Nat. Mater, 6, 183-191, 2007.
[4] A.A. Balandin, S. Ghosh, W. Bao, I. Calizo, D. Teweldebrahn, F. Miao, C.N. Lau, Superior thermal conductivity of single-layer graphene, Nano Lett. 8, 902–907, 2008
[5] C. Lee, X.D. Wei, J.W. Kysar, J. Hone, Measurement of the elastic properties and intrinsic strength of monolayer graphene, Science, 321, 385–388, 2008.
[6] Jvd. Brink, From strength to strength, Nat. Nanotechnol, 2007.
[7] W.S. Hummers, R.E. Offeman, Preparation of graphitic oxide, J. Am. Chem. Soc. 80, 1339, 1958.
[8] D.A. Dikin, S. Stankovich, E.J. Zimney, R.D, Piner, G.H.B. Dommett, G. Evmenenko, S.T. Nguyen, R.S. Ruoff, Preparation and characterization of graphene oxide paper, Nature, 448, 457-60, 2007.
[9] H. He, T. Riedl, A. Lerf, J. Klinowski, Solid-state NMR studies of the structure of graphite oxide, J. Phys. Chem. 100, 19954–19958, 1996.
[10] S. Stankovich, R. Piner, S.T. Nguyen, R.S. Ruoff, Synthesis and exfoliation of isocyanate-treated graphene oxide nanoplatelets, Carbon, 44, 3342–3347, 2006.
[11] S. Stankovich, R. Piner, X. Chen, N. Wu, S.T. Nguyen, R.S. Ruoff, Stable aqueous dispersions of graphitic nanoplatelets via the reduction of exfoliated graphite oxide in the presence of Poly (sodium 4-styrenesulfonate), J. Mater. Chem. 16, 155–158, 2006
[12] S. Stankovich S, D.A. Dikin, G.H.B Dommett, K.M. Kohlhaas, E.J. Zimney, E.A. Stach, R.D. Piner, S.T. Nguyen, R.S. Ruoff, Graphene based composite materials, Nature, 442, 282–286, 2006.
[13] S. Park, K.S. Lee, G. Bozoklu, W. Cai, S.T. Nguyen, R.S. Ruoff, Graphene oxide papers modified by divalent ions-enhancing mechanical properties via chemical cross-linking, ACS Nano, 2, 572–578, 2008.
[14] D. Li, M.B. Muller, S. Gilje, R.B. Kaner, G.G. Wallace, Processable aqueous dispersions of graphene nanosheets, Nature Nanotech, 3, 101-105, 2008.
[15] X. Sun, Z. Liu, K. Welsher, J. Robinson, A. Goodwin, S. Zaric, H.J. Dai, Nano-graphene oxide for cellular imaging and drug delivery, Nano Res. 1, 203-212, 2008.
[16] Z. Liu, J.T. Robinson, X.M. Sun, H.J. Dai, Pegylated nano-graphene oxide for delivery of water insoluble cancer drugs, J. Am. Chem. Soc. 130, 10876-10877, 2008.
[17] H.A. Becerril, J. Mao, Z. Liu, R.M. Stoltenberg, Z. Bao, Y. Chen, Evaluation of solution-processed reduced graphene oxide films as transparent conductors, ACS Nano, 2, 463-470, 2008
[18] X.Wang, L.J. Zhi, K. Mullen, Transparent, conductive graphene electrodes for dye-sensitized solar cells, Nano Lett. 8, 323-327, 2008
[19] X. Peng, X. Liu, D. Diamond, K.T. Lau, Synthesis of electrochemically-reduced graphene oxide film with controllable size and thickness and its use in super-capacitor, Carbon, 49, 3488-3496, 2011.
[20] K.S. Kim, Y. Zhao, H. Jang, S.Y. Lee, J.M. Kim, K.S. Kim, J. Ahn, P. Kim, J. Choi, B.H. Hong, Large-scale pattern growth of graphene films for stretchable transparent electrodes, Nature, 457, 706-710, 2009.
[21] Standard test for plane strain fracture toughness of metallic materials, ASTM E-399, American Society for Testing and Materials, Philadelphia, PA, 1987.
[22] D.K. Leung, M.Y. He, A.G. Evans, The cracking resistance of nanoscale layers and films, J. Mater. Res, 10, 1693-1699, 1995
[23] Y. Geng, S.J. Wang, J.K. Kim, Preparation of graphite nanoplatelets and graphene sheets, J. Colloid Interf. Sci. 336, 592-598, 2009.
[24] W.S. Hummers, R.E. Offeman, Preparation of graphitic oxide, J. Am. Chem. Soc. 80, 1339, 1958.
[25] X.Y. Lin , Q.B. Zheng, N. Yousefi, K.K. Yeung, X. Shen, J.K. Kim, Effects of reduction and size of graphene on mechanical and electrical properties of graphene oxide papers, 15th European Conference on Composite Materials, 2012.
[26] Progress in measuring fracture toughness and using fracture mechanics, fifth report of a special ASTM committee, materials research and standards,4, (1964), 107.
[27] F.A. Mcclintock, G.R. Irwin, Fracture toughness testing and its application, STP 381 (ASTM, Philadelphia, 1965), p. 84.
[28] P.C. Paris, G.C. Sih, Fracture toughness testing and its applications, STP 381 (ASTM, Philadelphia, 1965) p.30.
[29] A. Gupta, G. Chen, P. Joshi, S. Tadigadapa, P.C. Eklund, Raman scattering from high-frequency phonons in supported n-graphene layer films, Nano Lett. 6, 2667–2673, 2006.
[30] A.C. Ferrari, J.C. Meyer, V. Scardaci, C. Casiraghi, M. Lazzeri, F. Mauri, S. Piscance, D. Jiang,K.S. Novoselov, S. Roth, A.K. Geim, Raman spectrum of graphene and graphene layers, Phys. Rev. Lett. 97, 187401- 4, 2006.
[31] D. Graf, F. Molitor, K. Ensslin, C. Stampfer, A. Jungen, C. Hierold, L. Wirtz , Spatially resolved raman spectroscopy of single- and few-layer graphene, Nano Lett. 7, 238–242, 2007
[32] G. Venugopal, M.H. Jung, M. Suemitsu, S.J. Kim, Fabrication of nanoscale three dimensional graphite stacked junctions by focused-ion-beam and observation of anomalous transport characteristics, Carbon, 49, 2766-2772, 2011.
[33] M.A. Pimenta, G. Dresselhaus, M.S. Dresselhaus, L.G. Cançado, A. Jorio, R. Saito, Studying disorder in graphite-based systems by Raman spectroscopy, Phys. Chem. Chem. Phys. 9, 1276-1291, 2007.
[34] J.E. Srawley, W.F. Jr. Brown, Fracture toughness testing and its application. STP 381 (ASTM, Philadelphia, 1965), p. 133
[35] A. Omeltchenko, J. Yu,R. K. Kalia, P. Vashishta, Crack front propagation and fracture in a graphite sheet: A molecular-dynamics study on parallel computers, Physical review letters, 78, 2148-2151, 1997.
[36] Y. Liu, B. Xie, Z. Zhang, Q. Zheng, Z. Xu, Mechanical properties of graphene papers, J. of the Mechanics and Physics of Solids, 60, 591–605, 2012.
[37] X.Y. Lin, X. Shen, Q.B. Zheng, N. Yousefi, L. Ye,Y.W. Mai, J.K. Kim, Fabrication of highly-aligned, conductive, and strong graphene papers using ultralarge graphene oxide sheets, ACS Nano, 6, 10708–10719, 2012.